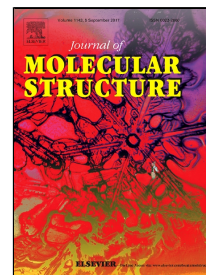


Accepted Manuscript

Hydrothermal syntheses, crystal structures, and photophysical properties of two 2D coordination polymers with mixed Ligands

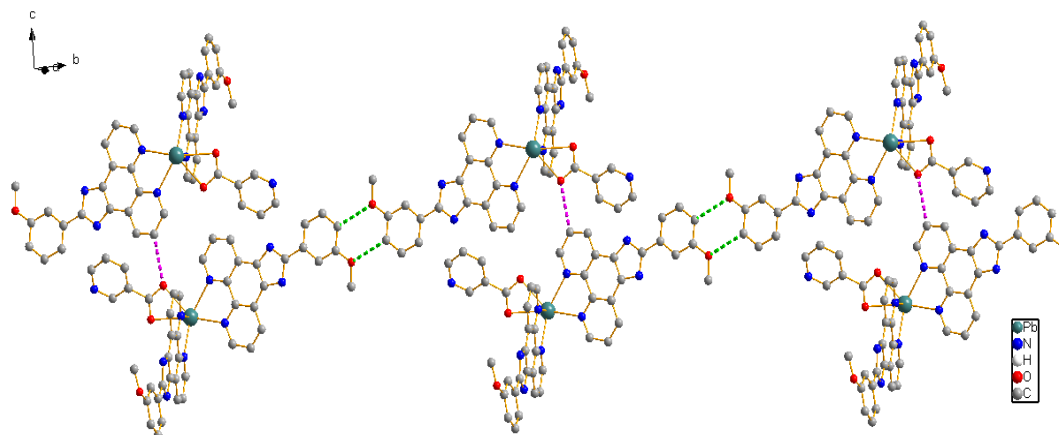
Li Yan, Chun-Ling Liu



PII: S0022-2860(17)30723-8
DOI: 10.1016/j.molstruc.2017.05.114
Reference: MOLSTR 23855
To appear in: *Journal of Molecular Structure*
Received Date: 11 December 2016
Revised Date: 23 May 2017
Accepted Date: 24 May 2017

Please cite this article as: Li Yan, Chun-Ling Liu, Hydrothermal syntheses, crystal structures, and photophysical properties of two 2D coordination polymers with mixed Ligands, *Journal of Molecular Structure* (2017), doi: 10.1016/j.molstruc.2017.05.114

This is a PDF file of an unedited manuscript that has been accepted for publication. As a service to our customers we are providing this early version of the manuscript. The manuscript will undergo copyediting, typesetting, and review of the resulting proof before it is published in its final form. Please note that during the production process errors may be discovered which could affect the content, and all legal disclaimers that apply to the journal pertain.

Graphical Abstract

Two complexes based on polycarboxylic acid and N-heterocyclic ligands have been synthesized and characterized by elemental analysis, IR, and X-ray diffraction analyses, where the solid-state fluorescence spectrum of compounds were have been studied.

Highlights

Two complexes were prepared and characterized by X-ray diffraction.

Weak interactions provide additional assembly forces.

Different intermolecular interactions lead to various crystalline aggregates.

Hydrothermal syntheses, crystal structures, and photophysical properties of two 2D coordination polymers with mixed Ligands

Li Yan*^{1,2}, Chun-Ling Liu^{1,2}

1. Key Laboratory of Preparation and Applications of Environmental Friendly Materials, Ministry of Education, Jilin Normal University, Siping, 136000, People's Republic of China

2. College of Chemistry, Jilin Normal University, Siping, 136000, People's Republic of China

Abstract

Two novel metal-organic coordination polymers $[\text{Cd}(\text{ipdt})(\text{m-BDC})\cdot 3\text{H}_2\text{O}]_n$ (**1**) and $[\text{Pb}(\text{mip})_2(\text{NTC})\cdot 2\text{H}_2\text{O}]_n$ (**2**) [ipdt = 2,6-Dimethoxy-4-(1H-1,3,7,8-tetraazacyclopenta[1]phenanthren-2-yl)-phenol, mip = 2-(3-methoxyphenyl)-1H-imidazo[4,5-f][1,10]phenanthroline, m-BDC = isophthalic acid, NTC = nicotinic acid] have been synthesized by hydrothermal reactions and characterized by elemental analysis, thermogravimetric (TG) analysis, infrared spectrum (IR) and single-crystal X-ray diffraction. Single-crystal X-ray diffraction reveals that **1** exhibits two-dimensional (2D) layer architecture, and **2** shows 1D chain architecture. TG analysis shows clear courses of weight loss, which corresponds to the decomposition of different ligands. The luminescent properties for the ligand ipdt, mip and complexes **1-2** are also discussed in detail, which should be acted as potential luminescent material.

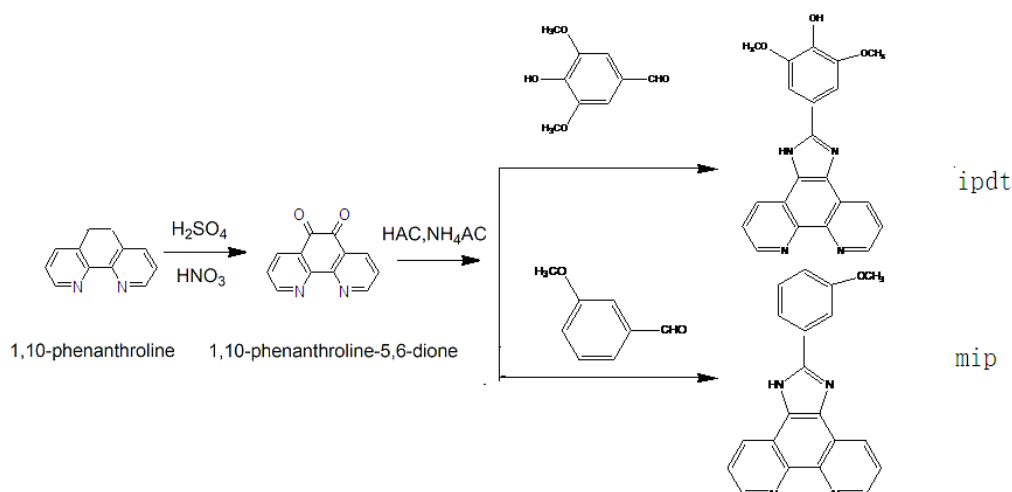
Keywords Cadmium, Lead, Crystal structures, Thermal stability analysis, Fluorescence

The project was supported by National Natural Science Foundation of China (No. 21406085), and the Science Development Project of Jilin Province of China (20130522071JH).

Corresponding author. Li Yan, E-mail: yanli820618@163.com

1. Introduction

During the past decades, the rational design and synthesis of novel metal-organic complexes have attracted intense interest owing to the realization of their potential use as materials in catalysis, porosity, sensors, magnetism, luminescence, molecular recognition and so on^[1-7]. In this aspect, considerable progress has been made on the theoretical prediction and network-based approaches for controlling the topology and geometries of the networks to produce useful functional materials. However, it is still a great challenge to predict the exact structures through controlling the factors that affect the framework formation, because the formation of metal-organic complexes are determined by several factors, such as the coordination nature of metal ions, coordination environment of metal nodes, ligand structures, pH value, structural characteristics of the polydentate ligands, solvents, templates, counterions, temperature and so on, may all play a role in determining the network structure of a compound^[8, 9]. Nowadays, the method of hydrothermal synthesis is widely used to synthesis novel crystal structures, because it can solve the problems of ligands solubility and enhance the reactivity of reactants in the crystallization process to obtain perfect crystal. Multidentate ligands such as poly-carboxylate and N-heterocyclic ligands are widely used in the rational design to obtain anticipated structures and desired properties^[10-13]. Our strategy of rational design and synthesis of coordination polymers is to employ a new designed long-conjugated unsymmetrical ligand ipdt (2,6-Dimethoxy-4-(1H-1,3,7,8-tetraaza-cyclopenta[1]phenanthren-2-yl)-phenol) and mip (2-(3-methoxyphenyl)-1H-imidazo[4,5-f][1,10]phenanthroline) (as shown in Scheme 1): in view of the following characteristics: (1) possess extended long-conjugated unsymmetrical aromatic system to provide supramolecular interactions; (2) possess two nitrogen atoms, which is similar with 2,2'-bipyridyl-like bidentate chelating molecules; (3) possess strong and rigidity of coordination ability to metal atoms. At this stage, combine N-heterocyclic ligands and anionic O-donor as mixed ligands with metal to design various architectures should be considered as an attractive design strategy. As far as we know, the investigation for the similar N-heterocyclic ligands is not enough, in especially it has not been reported for using ipdt, mip, isophthalic acid (m-BDC) and nicotinic acid (NTC) as mixed ligands to construct coordination polymers.



Scheme 1. The synthesis of ipdt and mip ligands

As for cadmium (II) ion, the chemistry of d^{10} metal clusters is of current interest not only because of their interesting structures but also their photoluminescent^[14, 15]. Up to now, the design and control over coordination compounds is mainly focused on the incorporation of *s*-, *d*-, and even *f*-block metals as coordination centers, whereas less attention has been paid to the *p*-block metals despite their important applications in electroluminescent devices and fluorescent sensors. Lead(II), as a heavy *p*-block metal ion, has a large radius and exhibits flexible coordination modes, which provides unique opportunities for the construction of novel coordination networks as well as photochemical and photo physical properties^[16].

In this paper, we use *m*-BDC and NTC for the second ligands to obtain two coordination polymers: $[\text{Cd}(\text{ipdt})(\text{m-BDC}) \cdot 3\text{H}_2\text{O}]_n$ (**1**) and $[\text{Pb}(\text{mip})_2(\text{NTC}) \cdot 2\text{H}_2\text{O}]_n$ (**2**). Both of the two complexes contain hydrogen bond interactions.

2. Experimental sections

2.1 Materials and physical measurements

The ligand ipdt and mip was prepared by the method according to the description in the literature procedures^[17]. All the other chemicals from commercial sources were of AR grade and used without further purification. The FT-IR spectrum was recorded on an Alpha Centauri FT-IR spectrophotometer using KBr discs in the $400\text{-}4000\text{ cm}^{-1}$ region. TG analysis was performed with a Diamond DSC thermal analyzer at the rate of $10\text{ }^\circ\text{C}/\text{min}$ rise of temperature in nitrogen

atmosphere. Crystal structures were determined on a Bruker SMART APEX II CCD X-ray diffractometer. Elemental analyses of C, H and N were performed on a PE-2400 elemental analyzer. Fluorescence spectra were recorded on a FLSP 920 Edinburgh fluorescence spectrometer.

2.2. Syntheses of 1–2

2.2.1. Synthesis of $[\text{Cd}(\text{ipdt})(\text{m-BDC})\cdot 3\text{H}_2\text{O}]_n$ (1**):** A mixture of $\text{Cd}(\text{NO}_3)_2\cdot 4\text{H}_2\text{O}$ (0.098 g, 0.3 mmol), ipdt (0.120 g, 0.3 mmol), m-BDC (0.100 g, 0.3 mmol) and H_2O (18 mL) was stirred at room temperature and adjusted the pH value to 6.0 with NaOH. We put the cloudy solution into a 30-mL Teflon-lined stainless vessel under autogenous pressure at 433 K for 72 h, and afterwards cooled to room temperature at a rate of 5 °C/ h. The yellow crystals of **1** were collected in 70% yield based on Cd. $\text{C}_{29}\text{H}_{26}\text{CdN}_4\text{O}_{10}$: calcd. C 49.55, H 3.73, N 7.97%; found: C 49.84, H 3.82, N 7.91%. IR (KBr, cm^{-1}): 3255(s), 3416(s), 1612(vs), 1521(vs), 1382(vs), 638(s), 561(m).

2.2.2. Synthesis of $[\text{Pb}(\text{mip})_2(\text{NTC})\cdot 2\text{H}_2\text{O}]_n$ (2**):** Complex **2** was synthesized by a procedure similar to that used for **1** except that the mixture was adjusted the pH value to 8.5, and heated the temperature under 453 K. Yellow crystals of **2** were collected in 85% yield based on Pb. $\text{C}_{46}\text{H}_{36}\text{N}_9\text{O}_6\text{Pb}$: calcd. C 54.27, H 3.56, N 12.38%; found: C 54.35, H 3.62, N 12.52%. IR (KBr, cm^{-1}): 3104(s), 3006(s), 1528(vs), 1393(vs), 1188(s), 1080(s), 732(s), 621(m).

2.3 X-ray crystallography

Single-crystal X-ray diffraction data were collected at room temperature with a Bruker SMART APEX II CCD diffractometer equipped with a graphite-monochromatized $\text{MoK}\alpha$ radiation ($\lambda = 0.71073 \text{ \AA}$) at 293(2) K in the range of $1.44 \leq \theta \leq 26.08^\circ$ for **1** and $1.50 \leq \theta \leq 26.03^\circ$ for **2**. Absorption corrections were applied using multi-scan technique and all the structures were solved by direct methods with SHELXS-97^[18] and refined with SHELXL-97^[19] by full-matrix least-squares techniques on F^2 . Non-hydrogen atoms were refined with anisotropic temperature parameters. Experimental details for crystallographic data and structure refinement parameters for **1** and **2** are listed in Table 1.

3. Results and discussion

3.1 Description of crystal structures

3.1.1 $[\text{Cd}(\text{ipdt})(\text{m-BDC})\cdot 3\text{H}_2\text{O}]_n$ (**1**)

The molecular structure of complex **1** is shown in Fig. 1. The 1D double-chain structure is

suggested in Fig. 2. The simplified 1D chain structure is suggested in Fig. 3, and the 2D layer structure linked by C–H···O hydrogen bonds is shown in Fig. 4. Selected important bond lengths and bond angles are given in Table 2.

As shown in Fig. 1, the asymmetric unit contains one Cd (II) atoms, one ipdt ligand, one m-BDC ligand, and three lattice water molecules. In **1**, the Cd (II) atom is hexa-coordinated with four carboxylate oxygen atoms from three distinct m-BDC ligands, and two nitrogen atoms donors from one chelating ipdt ligand, forming distorted octahedral geometry. The angle of O(2)–Cd(1)–N(1), N(1)–Cd(1)–N(2), N(2)–Cd(1)–O(7), and O(7)–Cd(1)–O(2) is 87.17, 70.78, 100.60 and 102.34°, and the sum is 360.89°. For the coordination environment of Cd(1), the Cd(1), O(2), N(1), N(2) and O(7) atoms define the basal plane, and O(1) and O(3) atoms occupy the apical axial positions. The equation of a plane is: $-4.2682(0.0456)x + 7.4613(0.0390)y + 13.6408(0.0151)z = 8.0454(0.0107)$. The deviation of atoms Cd(1), O(2), N(1), N(2) and O(7) to the plane is -0.4548, 0.2603, -0.0796, 0.2741, -0.8738, -2.5242 and 1.8265 Å, respectively. The bond distances of Cd–O in **1** are from 2.226 to 2.425 Å, and those of Cd–N bond distances fall in the 2.341 to 2.361 Å range, which are similar with the values reported^[20-23]. The N(O)–Cd–O(N) angles range are from 82.73 to 170.41°.

As showed in the Fig. 2, One m-BDC ligand coordinate to three Cd (II) ions through four carboxylic oxygen atoms in a mono-bridging and bidentate chelating fashion, which give rise to a 1D double-chain structure. It is interesting that in the unit of **1**, two type of rings formed: 8-membered ring, in which the angle of O(1)–Cd(1)–O(7) is 98.220°, and the distance of Cd···Cd is 3.952 Å; The 16-membered ring with the angle of O(1)–Cd(1)–O(2) is 90.150°, and The distance of Cd···Cd is 7.812 Å (Fig. 3); *N*-heterocyclic ligands ipdt are attached to both sides of this chain regularly, and the ligands on the same side are parallel nearly.

Hydrogen bonding interactions are usually important in the synthesis of supra-molecular architectures, and the most interesting aspect of the structure in **1** concerns the intermolecular N–H···O and C–H···O interactions. The existence of N4–H4A···O3 and C8–H8A···O3 hydrogen bonds interactions [H(4A)···O(4) = 1.99 Å, N(4)···O(3) = 2.806 Å and N4–H4A···O3 = 151°; H(8A)···O(3) = 2.52 Å, C(8)···O(3) = 3.353 Å and C8–H8A···O3 = 146°] lead the 1D chain to 2D structure, see Fig. 4. The two parallel ipdt ligands in the same side recognize each other through aromatic π - π stacking interaction with the face to face distance is 3.693 Å.

3.1.2[Pb(mip)₂(NTC)·2H₂O]_n (**2**)

The molecular structure is shown in Fig. 5, and the 1D chain structure is suggested in Fig. 6. Selected important bond lengths and bond angles are listed in Table 2.

As shown in Fig. 5, the asymmetric unit of complex **2** consists of one Pb (II) atom, two mip ligands, one NTC ligand, and two lattice water molecules. The Pb (II) atom is hexa-coordinated with four nitrogen atoms (N(2), N(3), N(6), N(7)) from two chelating mip ligands and two oxygen atoms from one chelating bidentate NTC, furnishing a distorted [PbN₄O₂] pentagonal bipyramidal geometry. For the coordination environment of Pb(1), the Pb(1), N6, N7, O1, O2, N3 atoms define the basal plane, and the N2 atom and the lone pair of electrons occupy the apical axial positions. The N(O)–Pb–O(N) angles range are from 73.02 to 156.80°. The bond distances of Pb–O in complex **2** are from 2.599 to 2.698 Å, and those of Pb–N bond distances fall in the 2.499 to 2.626 Å range, which are similar with the values reported^[24-27]. The most interesting factors are that contribute to the disposition of ligands around the lead with geometries are (1) holo-directed, in which the bonds to ligand atoms are distributed throughout the surface of an encompassing globe, and (2) hemi-directed, in which the bonds to ligand atoms are directed throughout only part of an encompassing globe^[28]. The coordination environment of Pb (II) in complex **2** is a good example of the hemi-directed coordination, in which the bonds to ligand atoms are directed throughout only part of the globe, that is, there is an identifiable gap (or void) in the distribution of bonds to the ligands.

Hydrogen bonding interactions are usually important in the synthesis of supramolecular architectures, and the most interesting aspect of the structure in **2** concerns the intermolecular C–H···O [H(43A)···O(4) = 2.36 Å, C(43)···O(4) = 3.236 Å and C(43)–H(43A)···O(4) = 158°] interactions, which helps in the construction of the 1D chain structure (Fig. 6).

In complex **1**, the coordination sphere of the Cd(II) ions are holo-directed, but the coordination sphere of the Pb(II) ions are hemi-directed in complex **2**. Coordination modes and the coordination sphere of the central metal ions are suggested in Fig. 7.

We can conclude that the diversity of coordination modes of dicarboxylates ligand result in the difference of structures in complexes **1** and **2**. Coordination modes (chelating bis-bidentate or bis-monodentate) usually raise the 1D chain or 1D double-chain structure, and diverse coordination modes (monodentate-bidentate or chelating/bridging bis-bidentate) usually raise the higher

dimensional crystal structures.

3.2 IR spectra

In **1**, the two peaks at 1612 and 1521 cm^{-1} correspond to the antisymmetric stretching of carboxyl, and the peak at 1383 cm^{-1} corresponds to the symmetric stretching of carboxyl. The $\Delta\nu$ ($\nu_{\text{as}}(\text{COO}^-) - \nu_{\text{s}}(\text{COO}^-)$) are 230 and 139 cm^{-1} , indicating that the carboxyls are bidentately and monodentately coordinated with Cd(II) atoms. In **2**, the strong absorption peaks at 1528 cm^{-1} is the antisymmetric stretching of carboxyl, and the absorption at 1393 cm^{-1} is the symmetric stretching of carboxyl. The separation is 135 cm^{-1} , which indicates the carboxyls adopt bidentate coordination mode. The IR results are good agreement with their solid structural features from the results of their crystal structures.

3.3 Thermal analysis

TG analysis was used to investigate the thermal stability of **1** and **2** (Fig. 8). As expected, TG analysis shows clear courses of weight loss, which corresponds to the decomposition of different ligands. Complex **1** exhibits three weight loss processes. First weight loss of 7.30% from 118 to 204 $^{\circ}\text{C}$ reveals the loss of the lattice water molecules (calcd. 7.68%). The second weight loss of 22.50% from 204 to 435 $^{\circ}\text{C}$ reveals the loss of the m-BDC ligands (calcd. 23.61%), and the last weight loss of 53.50 % from 435 to 631 $^{\circ}\text{C}$ corresponds to the loss of ipdt ligands (calcd. 52.92%); In **2**, the first weight loss of 3.05% from 252 to 263 $^{\circ}\text{C}$ corresponds to the loss of two lattice water molecules (calcd. 3.53%). The second weight loss in the temperature range of 352-453 $^{\circ}\text{C}$ can be ascribed to the release of NTC ligands (obsd 11.25%, calcd 12.08%), and the last weight loss of 65.10% from 453 to 676 $^{\circ}\text{C}$ corresponds to the loss of mip ligands (calcd. 64.04%). The final formation may be the metal oxide PbO.

3.4 Photoluminescent properties

Luminescent complexes are currently of great interest because of their various applications in photochemistry and photophysics. So in this study, we research the luminescence of complexes **1** and **2** (see Fig. 9 and 10). Complex **1** shows one strong emission band at 436 nm, and complex **2** shows one strong emission band at 578 nm (excitation at 320 nm). To further analyze the nature of these emission bands, the emission properties of ipdt as well as mip were also investigated under the same experimental conditions. The free ligand ipdt exhibits one emission band at 391 nm, and the ligand mip exhibits one emission band at 539 nm (excitation at 320 nm). The results suggest

that compared with free ligand, complex **1** is red-shifted by 45 nm relative to that of free ligand ipdt, and complex **2** is red-shifted by 39 nm relative to that of free ligand mip. Because the Cd(II) ion with d^{10} configuration is difficult to oxidize or to reduce, so the emission of **1** can be mainly be ascribed to the intra-ligand $\pi \rightarrow \pi^*$ transitions, namely ligand-to-ligand charge transfer (LLCT)^[29]. The emission of **2** can be attributed to a metal-centered transition involving the *s* and *p* metal orbitals, as proposed by Vogler et al^[30]. Additionally, the enhancement and the red shifts of luminescence emission maxima for **1** and **2** may be due to the chelating and bridging effects of the relevant ligands to the metal atoms, which effectively increase the rigidity and conjugation upon metal coordination and then affect the loss of energy by a radiationless pathway. However, the effect of the microenvironment between ligands and complexes on the luminescence properties still needs further investigations. Complexes **1** and **2** may be good candidate for potential photoluminescence materials, because it is highly thermally stable and insoluble in water and common organic solvents.

4. Conclusions

In conclusion, two unique complexes **1** and **2** have been synthesized by using plane multifunctional ligands ipdt, mip, m-BDC and NTC. It is noteworthy that non-covalent interactions ($\pi \cdots \pi$ interactions, H-bond and coordination bonds) can be one of the most powerful force for directing the supra-molecular structures. The results also present a feasible strategy for the construction of framework architectures by synthesis condition design, such as pH value, temperature, and so on. This material will give new impetus to the construction of novel functional material with potentially useful physical properties. Complexes **1-2** are very thermal stable and worthy of further study as candidate of potential photoluminescence material.

5. Supplementary materials

CCDC 943444 and 929590 contain the supplementary crystallographic data for **1** and **2**, respectively. These data can be obtained free of charge from the Cambridge Crystallographic Data Centre via www.ccdc.cam.ac.uk/ data request. cif.

Acknowledgement

We thank the National Natural Science Foundation of China (No. 21406085) and the Science Development Project of Jilin Province of China (20130522071JH) for financial support.

References

- [1] W.T. Chen, M.S. Wang, X. Lin, G.C. Guo, J.S. Huang, *Cryst. Growth Des.* 6, 2289 (2006)
- [2] J. L. C. Rowsell, O. M. Yaghi, *J. Am. Chem. Soc.* 128, 1304 (2006)
- [3] J. Xu, Z. Su, M.S. Chen, S.S. Chen, W.Y. Sun. *Inorg. Chim. Acta* 362, 4002 (2009)
- [4] H. Kwong, H. Yeung, W. Lee, W.T. Wong. *Chem. Commun.*, 46, 4841 (2006)
- [5] Z.Q. Zhang, R.D. Huang, Y.Q. Xu, C.W. Hu, *Chem. J. Chin. Univ.* 29, 1528 (2008)
- [6] J.W. Ye, J. Wang, J.Y. Zhang, P. Zhang, Y. Wang. *Cryst. Eng. Comm.* 9, 515 (2007)
- [7] A.J. Blake, N.R. Champness, T.L. Easun, D.R. Allan, H. Nowell, M.W. George, J.H. Jia, X.Z. Sun, *Nature Chem* 2, 688 (2010)
- [8] J.P. Zhang, X.M. Chen, *Chem. Comm.* 16, 1689 (2006)
- [9] J. Yang, J.F. Ma, Y.Y. Liu, J.C. Ma, S.R. Batten, *Inorg. Chem.* 46, 6542 (2007)
- [10] X.L. Xu, Y. He, J.H. Pang, Z.G. Kong, *Chin. J. Inorg. Chem.* 27, 2279 (2011)
- [11] X.L. Xu, Y. He, S. Ma, N.S. Weng, *Chin. J. Inorg. Chem.* 28, 851 (2012)
- [12] Y.J. Huang, L. Ni. *J. Inorg. Organomet. Polym.* 21, 97 (2011)
- [13] L. Yan, C.B. Li, D.S. Zhu, L. Xu, *J Inorg. Organomet. Polym.* 22, 395 (2012)
- [14] H. Chen, H. Xu, G.X. Liu, X.M. Ren, *Chem. J. Chin. Univ.* 25, 1508 (2009)
- [15] C. Guo, X.J. Kong, X.M. Ren, G.X. Liu, *Chem. J. Chin. Univ.* 25, 1452 (2009)
- [16] Q.Y. Liu, L. Xu, *Eur. J Inorg. Chem.* 2006, 1621 (2006)
- [17] Q.L. Zhang, J.H. Liu, X.Z. Ren, H. Xu, Y. Huang, J.Z. Liu, L.N. Ji, *J Inorg. Biochem.* 95, 195 (2003)
- [18] G.M. Sheldrick, SHELXS 97, Program for the Solution of Crystal Structure (University of Göttingen, Germany, 1997)
- [19] G.M. Sheldrick, SHELXS 97, Program for the Refinement of Crystal Structure (University of Göttingen, Germany, 1997)
- [20] W. Q. Geng, X. L. Li, J. H. Yin, H. P. Zhou, J. Y. Wu, Y. P. Tian, *Inorg. Chem. Comm.* 13, 1285 (2010)
- [21] J. Zhang, B. Li, X. Wu, H. Yang, W. Zhou, X. Meng, H. Hou, *J. Mol. Struct.* 984, 276 (2010)
- [22] M. Hu, X.G. Yang, Q. Zhang, L.M. Zhou, S.M. Fang, C.S. Liu, *Z. Anorg. Allg. Chem.* 637, 480 (2011)
- [23] S.L. Li, Y.Q. Lan, J.F. Ma, J. Yang, G.H. Wei, L.P. Zhang, Z.M. Su, *Cryst. Growth Des.* 8, 680 (2008)
- [24] Q.Y. Liu, L. Xu, *Eur. J. Inorg. Chem.* 2006, 1621 (2006)
- [25] C.X. Li, J. Wang, C.B. Liu, G.B. Che, X.Y. Li, X.C. Wang, *Chin. J. Inorg. Chem.* 25, 2213 (2009)
- [26] F. Marandi, R. Rutvand, M. Rafiee, J.H. Goh, H.K. Fun, *Inorg. Chim. Acta* 363, 4003 (2010)

- [27] Y.J. Shi, G.Q. Jiang, Y.H. Zhang, X.Z. You, Appl. Organometal. Chem. 18, 89 (2004)
- [28] X.L. Wang, Q. Gao, Y.Q. Chen, G.C. Liu, A.X. Tian, Z.H. Kang, Z Anorg Allg Chem 637, 144 (2011)
- [29] M. Hu, X.G. Yang, Q. Zhang, L.M. Zhou, S.M. Fang, C.S. Liu, Z Anorg Allg Chem 637, 478 (2011)
- [30] P.C. Ford, A. Vogler, Acc Chem Res 26, 220 (1993)

Table 1Crystal data and details for **1** and **2**

Compound	1	2
Empirical formula	C ₂₉ H ₂₆ CdN ₄ O ₁₀	C ₄₆ H ₃₆ N ₉ O ₆ Pb
Formula weight	702.94	1018.03
Crystal system	monoclinic	monoclinic
space group	<i>C2/c</i>	<i>P2(1)/n</i>
<i>a</i> (Å)	20.296(5)	10.623(4)
<i>b</i> (Å)	22.010(6)	16.771(7)
<i>c</i> (Å)	14.836(4)	22.946(1)
β (°)	115.144(4)	92.771(1)
Volume (Å ³)	6000(3)	4083(5)
<i>Z</i>	8	4
Density (Mg/m ³) (calculated)	1.556	1.656
Absorption coefficient (mm ⁻¹)	0.791	4.195
<i>F</i> (000)	2848	2020
Crystal size (mm ³)	0.41 x 0.32 x 0.30	0.34 x 0.30 x 0.25
Theta range (°)	1.4426.08	1.5026.03
Reflections collected	16187	29899
Unique reflections [<i>R</i> _{int}]	5895 [0.040]	8000 [0.034]
Goodness-of-fit on <i>F</i> ²	1.035	1.018
Final <i>R</i> indices [<i>I</i> > 2σ(<i>I</i>)]	<i>R</i> 1 = 0.046 <i>wR</i> 2 = 0.136	<i>R</i> 1 = 0.031 <i>wR</i> 2 = 0.074
<i>R</i> indices (all data)	<i>R</i> 1 = 0.069 <i>wR</i> 2 = 0.153	<i>R</i> 1 = 0.043 <i>wR</i> 2 = 0.079
Largest difference peak and hole (e. Å ⁻³)	1.470, -0.586	1.491, -0.514

Table 2Selected bond lengths [\AA] and bond angles [$^\circ$] for **1**

bond	Dist.	bond	Dist.
Cd(1)–O(1)	2.257(4)	Cd(1)–O(2)	2.367(3)
Cd(1)–O(3)	2.425(4)	Cd(1)–O(7)	2.226(4)
Cd(1)–N(1)	2.341(4)	Cd(1)–N(2)	2.361(4)
Angle	($^\circ$)	Angle	($^\circ$)
O(1)–Cd(1)–O(3)	144.50(12)	O(2)–Cd(1)–O(3)	54.78(12)
O(7)–Cd(1)–O(1)	98.21(15)	O(7)–Cd(1)–O(3)	95.05(13)
O(1)–Cd(1)–O(2)	90.15(13)	O(7)–Cd(1)–O(2)	102.34(14)
N(1)–Cd(1)–O(3)	89.49(14)	O(7)–Cd(1)–N(1)	170.41(14)
O(1)–Cd(1)–N(1)	82.73(14)	N(1)–Cd(1)–O(2)	87.17(15)
O(7)–Cd(1)–N(2)	100.60(15)	O(1)–Cd(1)–N(2)	117.74(14)
N(2)–Cd(1)–O(2)	140.54(13)	N(2)–Cd(1)–O(3)	91.66(13)
N(1)–Cd(1)–N(2)	70.78(14)		

Table 3Selected bond lengths [\AA] and bond angles [$^\circ$] for **2**

bond	Dist.	bond	Dist.
Pb(1)–O(1)	2.698(3)	Pb(1)–O(2)	2.599(3)
Pb(1)–N(2)	2.499(3)	Pb(1)–N(3)	2.568(3)
Pb(1)–N(6)	2.626(3)	Pb(1)–N(7)	2.596(3)
Angle	($^\circ$)	Angle	($^\circ$)
O(2)–Pb(1)–O(1)	49.20(8)	O(2)–Pb(1)–N(6)	132.08(9)
N(7)–Pb(1)–O(2)	75.27(9)	N(3)–Pb(1)–O(2)	117.69(9)
N(2)–Pb(1)–O(2)	73.02(10)	N(2)–Pb(1)–O(1)	81.98(10)
N(3)–Pb(1)–O(1)	80.23(9)	N(7)–Pb(1)–O(1)	124.47(9)
N(6)–Pb(1)–O(1)	156.80(10)	N(2)–Pb(1)–N(3)	65.15(10)
N(2)–Pb(1)–N(7)	81.01(10)	N(3)–Pb(1)–N(7)	135.39(10)
N(2)–Pb(1)–N(6)	77.72(11)	N(3)–Pb(1)–N(6)	81.13(10)
N(7)–Pb(1)–N(6)	63.19(10)		

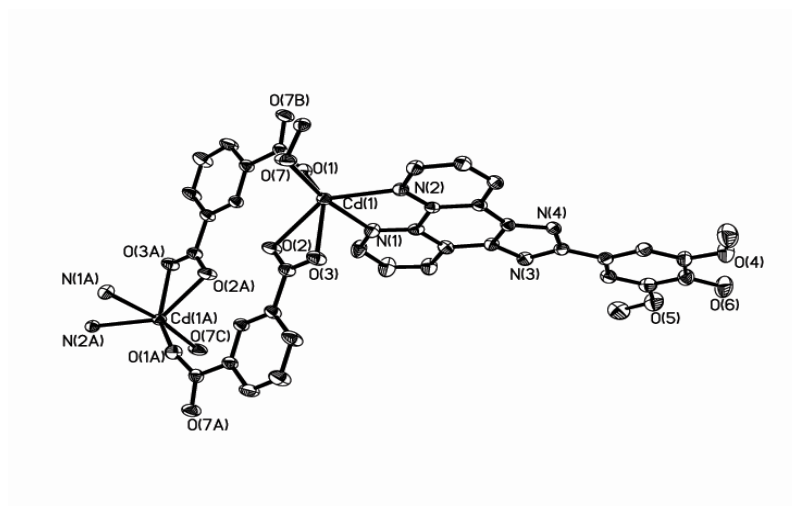


Fig. 1 The molecular structure of complex **1** (*hydrogen atoms were omitted*)

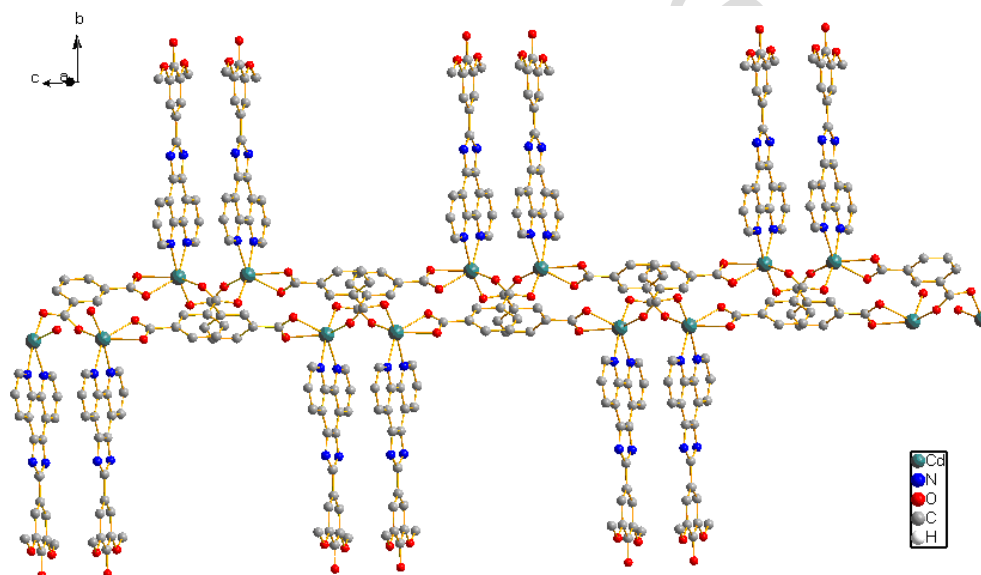


Fig. 2 1D double chain structure of complex **1** (*hydrogen atoms were omitted*)

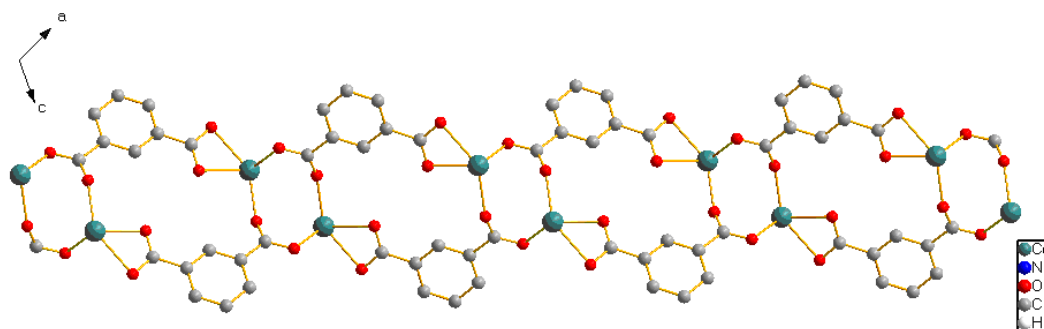


Fig. 3 The simplified chain structure of complex **1** (*hydrogen atoms were omitted*)

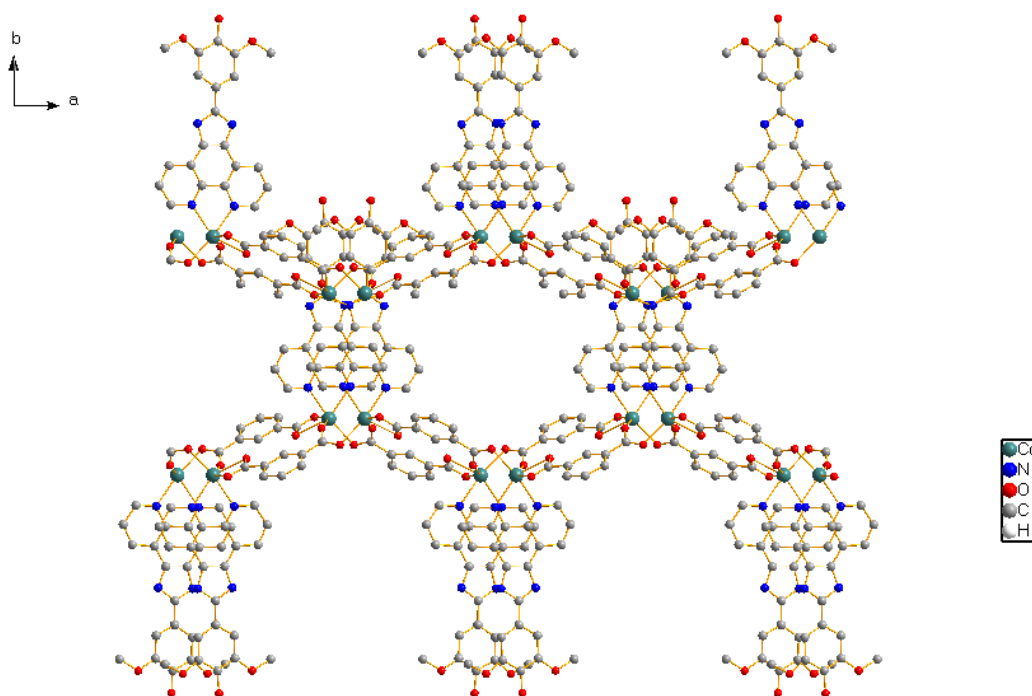


Fig. 4 2D layer structure of complex 1 linked by C-H \cdots O hydrogen bonds (*dotted lines represent hydrogen bonds*)

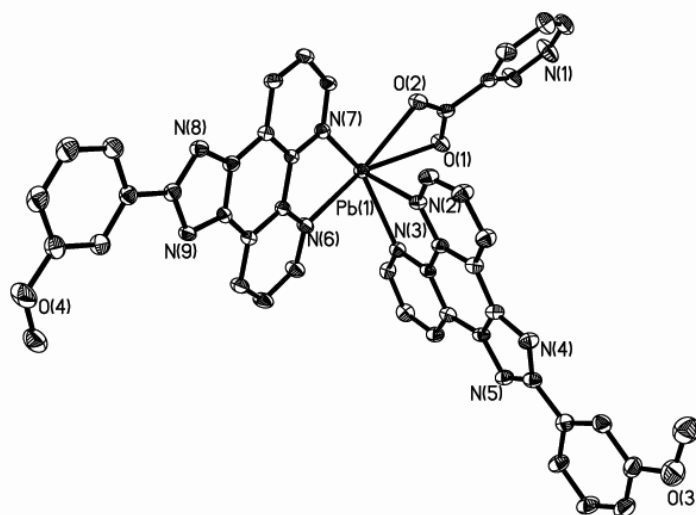


Fig. 5 The molecular structure of complex 2 (*hydrogen atoms were omitted*)

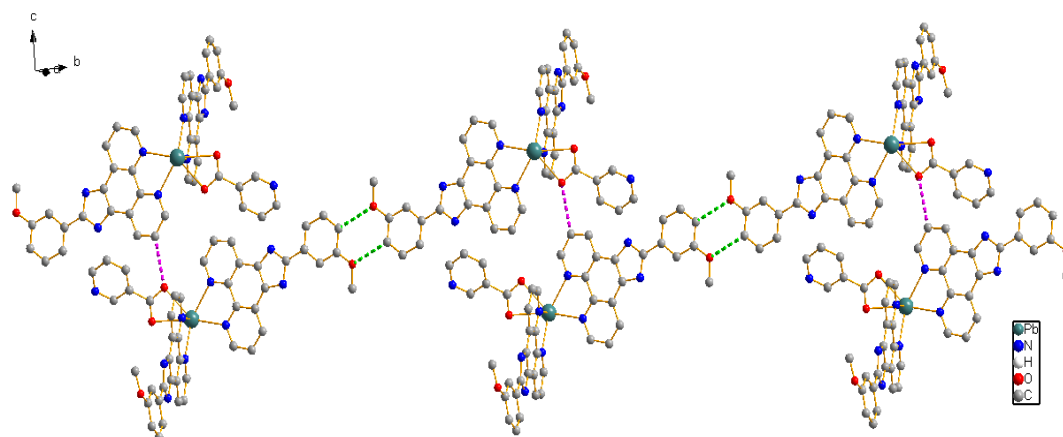


Fig. 6 1D arm-shaped chain structure of complex **2** (hydrogen atoms were omitted)

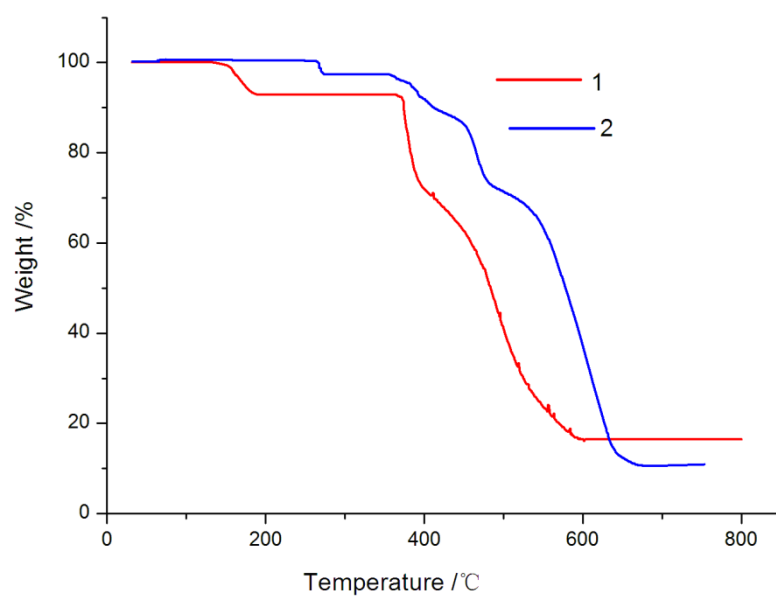


Fig. 7 TG curves of complexes **1** and **2**

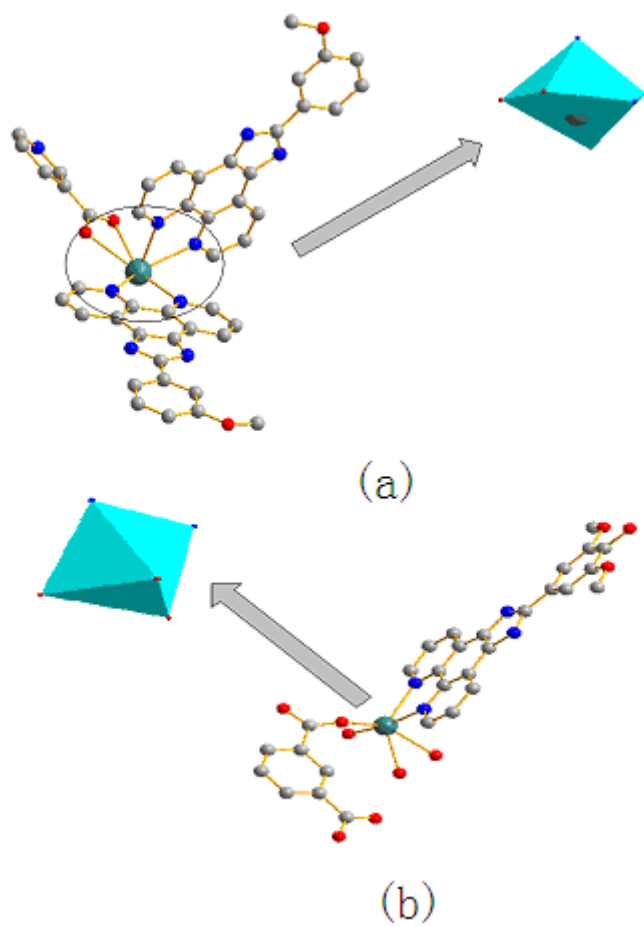


Fig. 8 Coordination modes and sphere of the central metal ions in complex **1** (a) and complex **2** (b)

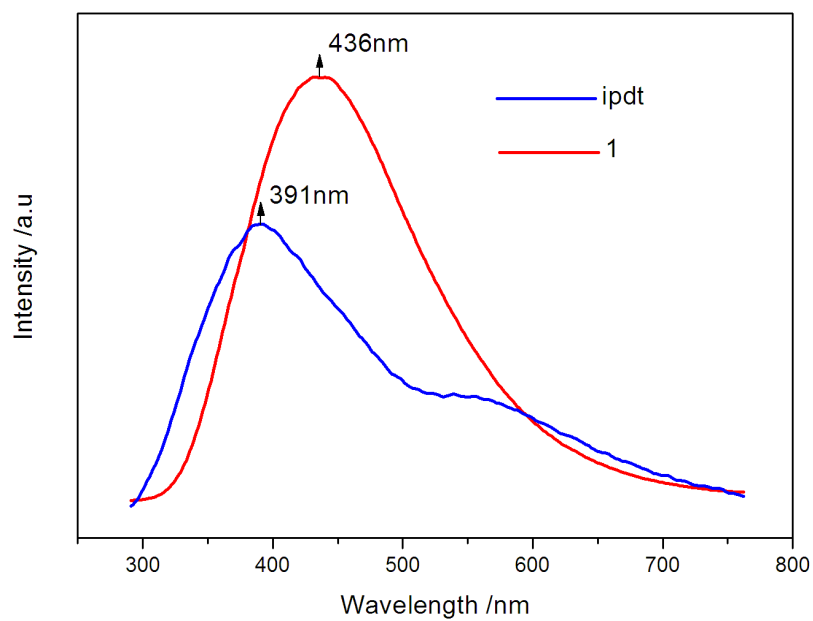


Fig. 9 Luminescent spectrum of complex 1 and ipdt ligand in solid state at room temperature

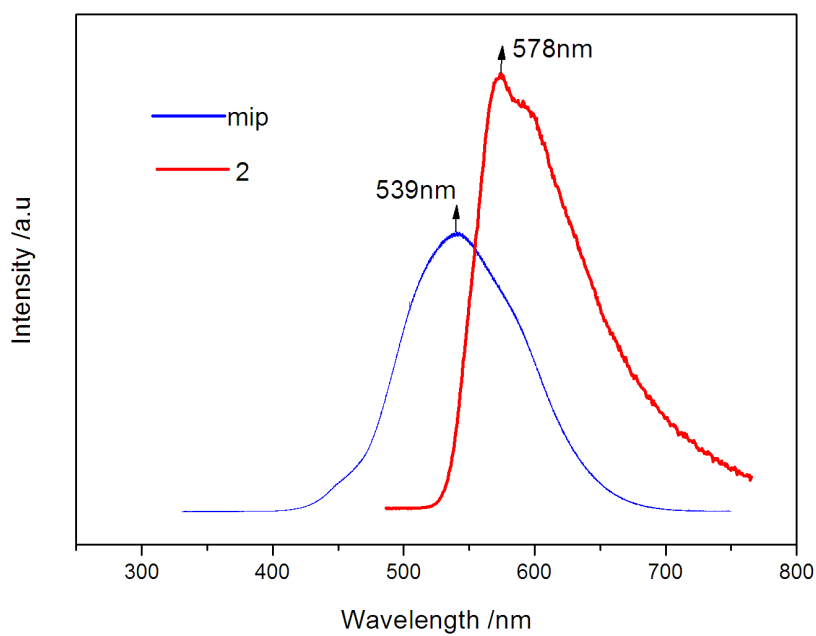


Fig. 10 Luminescent spectrum of complex 2 and mip ligand in solid state at room temperature